Response of concrete cast in permeable moulds to severe heating

16th November 2017

Response of concrete cast in permeable moulds to severe heating

O Richards MEng (hons)

Researcher, University of Bath, Bath, BA2 7AY

Ieuan Rickard MEng (hons)

PhD Candidate, School of Engineering, University of Edinburgh, Edinburgh, EH9 3JG

Dr J Orr MEng(hons) PhD CEng MIStructE FHEA

University Lecturer in Concrete Structures, University of Cambridge, Cambridge, CB2 1PZ

Professor L Bisby BEng MSc(Eng) PhD PEng CEng FIStructE FIFireE FIESIS

School of Engineering, University of Edinburgh, Edinburgh, EH9 3JG

Abstract

This paper evaluates the effect that a permeable mould, such as would be used to create fabric-formed concrete, may have on the heat-induced explosive spalling performance of cast concrete, using a novel experimental fire testing method and supported by scanning electron microscopy. Recent research suggests that a concrete cast using fabric formwork will gain durability enhancements at the cast surface that may negatively affect pore-pressure expulsion during severe heating. Six concrete samples were cast using high strength concrete including silica fume and tested using the University of Edinburgh's Heat-Transfer Rate Inducing System (H-TRIS), receiving thermal loading on one surface. Three samples were cast in permeable moulds, formed using a Huesker HaTe PES 70/70 single layer woven geotextile with a characteristic opening size (O_{90}) of $0.1x10^{-3}$m. Three samples were cast in conventional impermeable timber moulds. The tests showed no conclusive evidence of differences in thermal profile or differential thermal deflections between the two casting methods; no occurrences of heat-induced explosive spalling were observed for either casting method. However, scanning electron microscopy undertaken on additional samples showed that the test face of samples cast in permeable moulds were over four times less porous compared to their impermeably cast equivalents. This could increase the risk of spalling of samples, particularly in cases where pore-pressure spalling dominates the material response. However, additional fire testing using H-TRIS is needed under a range of heating and loading conditions, before definitive conclusions on the spalling propensity of fabric-formed concrete can be made.

1 Introduction

Detailed structural optimisation of concrete structures can yield material savings in the order of 40% (Orr et al., 2011). Such savings can be achieved, for example, by using flexible, permeable, fabric moulds that allow optimised forms to be cast. The permeability of fabric moulds (which are typically made using geotextiles) allows excess water and trapped air to escape, resulting in a more durable surface finish with a denser and more tightly packed microstructure (Orr et al., 2013). In addition, fabric formwork is reusable in most cases, with the fabric geometry able to form a different element by an adjustment of its specific tension and clamping (Chandler and Pedreschi, 2007).

Permeability is widely believed to influence the propensity for heat-induced explosive concrete spalling (Klingsch, 2014). Since permeable formwork typically reduces the porosity of the cast face, the extent to which a fabric formed surface layer may alter the tendency for a concrete sample to spall is unknown. Indeed, like-for-like tests performed on the same concrete mix but with differing surface porosity can help to unpick the relative importance of pore-pressure effects versus differential thermal effects as drivers for heat-induced spalling of concrete.

Severe thermal exposure testing undertaken at the University of Edinburgh using the bespoke Heat-Transfer Rate Inducing System (H-TRIS) aimed to observe potential differences in propensity for heat induced spalling, whilst also observing internal temperatures and differential thermal displacements to evaluate the effects of casting with a permeable mould on high temperature performance of concrete. Further testing involved a study of the pore structure of fabric and timber-formed cast concrete surfaces using a scanning electron microscope (SEM).

2 Literature review

2.1 Flexible formwork

Fabrics have been an integral part of permeable mould formwork since the 19th century. It wasn't until the late 1980s, however, that research into synthetic fabrics resulted in high strength, tear resistant, and economical materials for this purpose. This led in turn to new methods of concrete construction for offshore, hydraulic, and coastal engineering environments (Veenendaal et al., 2011). More recent research into the use of permeable moulds has explored its use for structural optimisation, geometric form finding, and enhanced constructability (Hawkins et al., 2016). Figure 1 shows an example of a structurally optimised beam designed to minimise material and self-weight whilst maximising flexural strength.

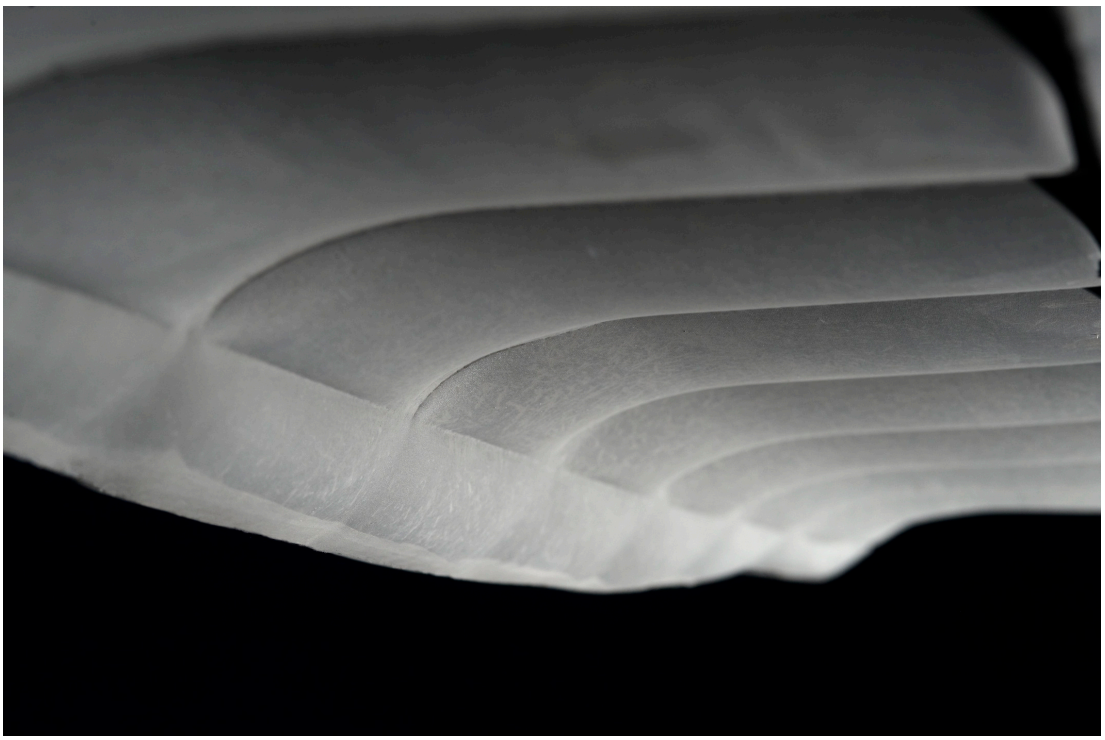

Figure 1: Fabric formed concrete beam optimised for flexural strength.

2.1.1 Concrete properties

When cast into permeable formwork, excess water in the concrete in a zone of approximately 0-15mm from the cast surface can escape (Orr et al., 2013). The water to cement ratio in this zone is thereby reduced (by around 35%, depending on the fabric porosity (Orr et al., 2011, Frank, 2015)). This provides a localised increase in surface strength of as much as 80% (Frank, 2015), a higher density, and lower permeability (Orr et al., 2013). Furthermore, any air trapped in the formwork is also able to escape (Chandler and Pedreschi, 2007). Combined, these two mechanisms result in a significantly improved quality of the cast face.

The local increase in strength and reduction in permeability at the surface of the cast material also leads to improvements in durability. Orr et al. (2013) showed 50% average reductions in carbonation and chloride ingress, for fabric formed concrete, reinforcing similar research carried out by Price (2000) on controlled permeability formwork (CPF). If there are smaller pores and a reduced volume of interconnected pores present in the concrete surface layer, it is anticipated to increase the propensity for heat-induced explosive concrete spalling. A reduction in porosity will prevent the expulsion of gases (including pore moisture) through the surface layer at high temperatures, thereby potentially increasing the likelihood of spalling, further exacerbated by high strength concrete which is known to be more susceptible to spalling (Khoury, 2000).

2.2 Spalling

Khoury (2000) described spalling as the process of concrete breaking off from a structural member, during high temperature states, in a violent or non-violent nature. Although research has been conducted on spalling since at least the 1910s (Klingsch, 2014), spalling remains an incompletely understood phenomenon within

the scientific community – and is currently impossible to predict with confidence. An example of severe heat-induced concrete spalling is shown in Figure 2, where only the spalled area was exposed to heating during the test. A loss of structural material is evident, which reduces the volume of the element and could result in failure through loss of cross section or loss of thermal protection to the internal steel reinforcement.

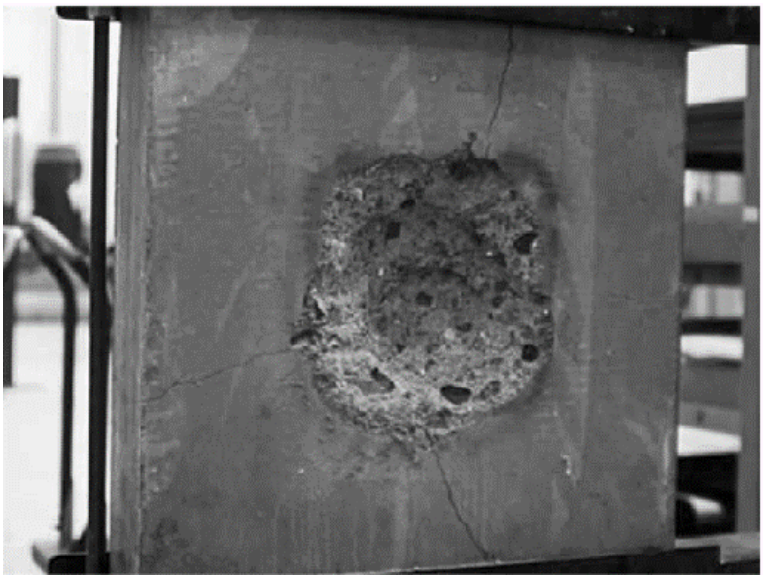

Figure 2: ***Severe heat-induced explosive spalling of a concrete sample locally exposed to elevated temperature (Hertz, 2003b).***

According to Jansson (2008), prominent researchers in the late 20th Century Meyer-Ottens (1972) and Copier (1979) hypothesised that the probability of spalling is low if the moisture content of concrete is also low. Mindeguia et al. (2011) proposed that free and physically bound water holds the core responsibility over the development of internal pore pressures from elevated temperatures. Considering moisture as an important factor affecting the propensity for concrete spalling, it is therefore clearly detrimental to have a large amount of free water within a sample.

The Moisture Clog Model originally developed by Harmathy (1965) describes one of two widely accepted theoretical mechanisms for spalling. At elevated temperatures, a plane of fully saturated concrete is expected to form within the concrete specimen, as a result of vaporisation of pore water within the concrete, restricting the movement of steam out of the sample. This causes pore pressures within the concrete to rise. Once the tensile strength of the concrete is exceeded locally, spalling may occur (Jansson, 2013). By cutting specimens shortly after they been tested at high temperature Jansson (2013) demonstrated that a moisture clog layer was visible, which partly validated this explanation of pore pressure as a factor influencing spalling. Although the mechanism has not been definitively proven and the research community has put forward various alternative mechanisms (Khoury, 2000), the Moisture Clog theory is still regarded as relevant to explaining the phenomenon of spalling. The other key mechanism involves differential thermal stresses which are generated as the concrete surface heats and tries to expand, whereas the cooler concrete within the core remains cool; this generates differential thermal stresses which are also thought to influence spalling. Indeed many researchers now feel that Thermal Stress Spalling is more important than Pore Pressure Spalling in many applications (Zhang and Davie, 2013).

In addition to moisture content, there are many further factors expected to influence spalling. These varied and complex factors range from the mix properties of the cast concrete to the geometry of the specimen, external loading, restraint conditions, and the heating rate (Jansson, 2008).

A brief explanation of spalling related factors directly linked to the testing undertaken in the current paper are given in Table 1; the risk related to spalling is after Klingsch (2014).

141

142 **Table 1: Spalling factors and their associated risk (after Klingsch, 2014)**

Factor	Risk of spalling	Influence
Silica fume content	Very high	Testing by Hertz (2003) showed that the mixes between the cement grains leads to a higher propensity for explosive spalling.
Permeability	High	Directly affects the release of vapour pressures, and so with low permeability, gasses have difficulty escaping and the risk of spalling is increased.
Type of aggregate	Variable	Limestone is based on carbonates and has a higher heat capacity with low thermal expansion, compared to siliceous aggregates (Kodur and Phan, 2007).
Aggregate size	Moderate	Connolly (1995), cited by Klingsch (2014), states that larger aggregates moderately increase the risk of spalling due to such mixes having inferior surface/mass ratios.
Compressive strength	High	Permeability reduces with increased strength/density from a lower water/cement ratio, thus increasing the risk of explosive spalling (Kodur and Phan (2007).

143

144 Extensive research has been performed with the aim of minimising, and ultimately
145 preventing, heat-induced explosive concrete spalling (Zeiml et al., 2006). A common
146 method of spalling mitigation is by adding polypropylene (PP) anti-spalling fibres to a
147 concrete mix. Research suggests that at around 170°C the PP fibres melt, creating
148 channels through the concrete matrix and altering the microstructure by increasing its
149 porosity (Klingsch, 2014). Water vapour formed during high temperature can
150 therefore be more easily expelled, and the build-up of internal pore pressures is
151 reduced (Lura and Terrasi, 2014). It is noteworthy that this theory of PP anti-spalling
152 fibres' mechanism of functioning has yet to be fully validated, and it remains a topic
153 of some controversy.

154 ## 2.3 Structural fire testing

155 Full-scale fire tests of real buildings are rare, with a few notable exceptions such as
156 Cardington (Kirby, 1997). In general engineers must rely on smaller-scale standard
157 furnace testing to develop design guidance for spalling. In 1918, the first

158 standardised test method was published: ASTM C19, now redesignated as ASTM
159 E119 (2016) (Grosshandler, 2002) which included the innovation of a prescribed
160 time-temperature curve (Lawson et al., 2009). Despite fundamental pitfalls in the
161 ability of ASTM E119 (2016) to demonstrate/validate the fire resistance of real
162 structures in real fires, its fundamental testing formula remains essentially unchanged
163 since 1918 (Maluk and Bisby, 2012). The current British Standard BS EN 1992-1-2
164 (2004) for fire safety structural design of concrete structures has been developed
165 from the same principles of ASTM E119 (2016) and so also contains time-
166 temperature curves.

167 *2.3.1 Furnace testing limitations*

168 Standard fire resistance testing in furnaces has some significant limitations.
169 Researchers sometimes test multiple specimens simultaneously, leading to over-
170 instrumentation while the exposed thermal environment is partly ignored (Maluk et
171 al., 2012). Due to the comparatively high cost for furnace testing, a limited number of
172 tests can typically be performed, which results in an inability to perform repeat testing
173 or any statistical analysis, and making a reliability-based approach to design
174 impossible (Maluk et al., 2012). In addition, furnace testing has comparatively poor
175 repeatability, and the thermal energy that the specimen absorbs over time is only
176 indirectly controlled by making measurements of gas temperatures within the
177 furnace, as opposed to heat absorbed into the test samples (Maluk and Bisby, 2012).
178 It can thus be difficult to accurately quantify the thermal loading a specimen receives
179 within a furnace (Maluk et al., 2012).

180 *2.3.2 Heat-Transfer Rate Inducing System (H-TRIS)*

181 A novel thermal testing method has been developed at the University of Edinburgh
182 (Maluk et al., 2016) called The Heat Transfer Rate Inducing System (H-TRIS) (Figure

3). This consists of four high performance propane-fired radiant heaters (to provide thermal loading), mounted on a mechanical linear motion system. When testing using H-TRIS the thermal exposure is controlled directly by controlling the heat flux the specimen is exposed to during testing as opposed to the controlling the temperature within the furnace in standard tests (Hulin et al., 2015). A heat flux gauge is used to measure and calibrate the incident heat flux from the radiant panels at the surface of the tested element, and the position of the radiant panels from the sample face is varied so as to simulate the desired time-history of thermal gradients within the sample. If desirable to compare results to those of standard furnace tests, the thermal exposure equivalent to the thermal exposure that samples experienced during a specific standard furnace test can be calculated. This is done using through thickness temperatures from samples tested in the furnace and an inverse heat transfer model; the result being the equivalent incident heat flux versus time curve. Before testing, the incident heat flux is measured using a Schmidt-Boelter heat flux gauge at different offset distances from the radiant panels. Thermal exposure is then controlled by controlling the distance between the radiant panels and sample in accordance with this calibration

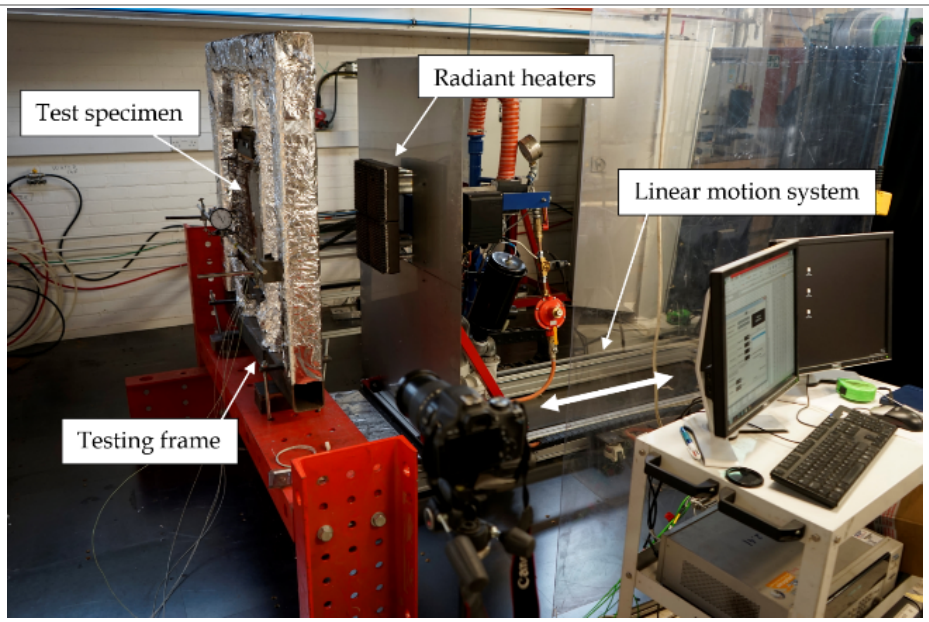

Figure 3: An overview of the H-TRIS testing apparatus at The University of Edinburgh.

3 Test methodology

To investigate and compare the spalling behaviour of concrete cast in permeable versus impermeable moulds, a total of six prismatic concrete test samples, with dimensions 500mm x 200mm x 45mm, were cast for testing using the H-TRIS methodology and apparatus.

3.1 Sample construction

Three samples were cast with permeable formwork on one face, and three were cast within impermeable moulds. Two additional samples (one of each mould type) were cast for later analysis using scanning electron microscopy (SEM). Nine 100mm cubes were also cast alongside the samples for mix characterisation purposes. All test samples were internally instrumented with five 0.3mm diameter welded tip insulated fibreglass (Type K) thermocouples (see Figure 4), with their tips carefully placed (+/- 2mm) at depths of 2mm, 5mm, 10mm, 22mm and 45mm from the face exposed to heating. These were placed using a thermocouple tree arrangement (as shown in Figure 4) which was cast inside the samples during casting operations. The

fifth thermocouple was placed on the back face of each specimen during testing, covered by ceramic insulation and sealed in place using aluminium tape.

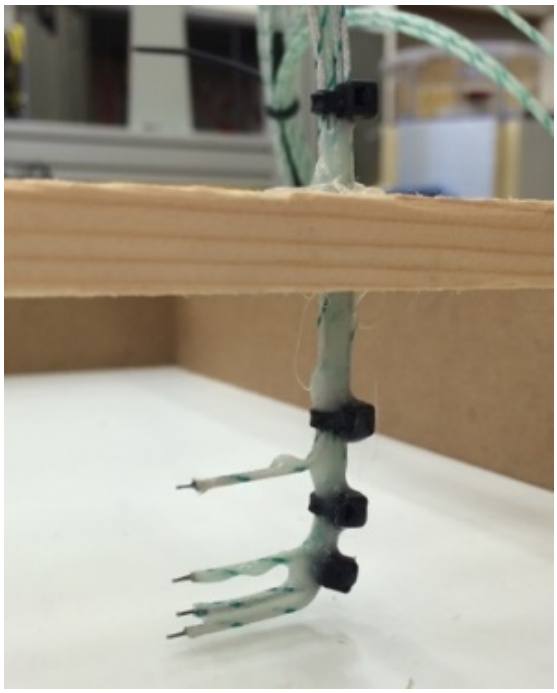

Figure 4: Thermocouple tree restrained in place within the formwork prior to casting the samples.

The mix design used in the current study (see Table 2) had a 28-day design compressive cube strength of 60MPa. This compressive strength was chosen as it is a realistic strength that is used in permeable concrete formwork building construction. All concrete was mixed in the Concrete Laboratory at the University of Bath, following The Silica Fume Association (2011) guidance for casting with silica fume. All samples and cubes were cured in accordance with BS EN 13670 (2009b). All samples were weighed 48 hours after casting. The samples were transported to Edinburgh and tested 90 days after casting. The fabric used was HaTe PES 70/70, with a characteristic opening size of 0.1×10^{-3} m.

234

Table 2: Concrete mix design

Material	Amount
Cement CEM I 42.5 R (kg/m^3)	400
Coarse aggregates (4-20mm) (kg/m^3)	1000
Fine aggregates (0-4mm) (kg/m^3)	840
Superplasticiser (l/m^3)	4
Water (l/m^3)	180
Silica fume (kg/m^3)	40
Unit weight, $\gamma_{c,\ mix\ A}$ (kg/m^3)	2464
28 day compressive strength, $f_{c,28}$ (MPa)	60
Water/cement ratio	0.41

235

236 ## 3.2 Test setup

237 The test set up for the spalling tests is shown in Figure 5 and Figure 6. Specimens
238 were placed into a supporting test frame, with cork placed underneath each concrete
239 sample to prevent them from moving during heating. However, the concrete
240 specimens were not mechanically restrained, thus allowing free thermal expansion
241 and bowing during testing.

242 Research has shown that the application of an appropriate external load or restraint
243 can influence spalling (Hertz and Sørensen, 2004, Rickard et al., 2017). However,
244 since this is a pilot study, the parameters being investigated were kept to a minimum
245 and a loading frame was not used for these samples.

246 A displacement gauge was attached at the centre of the back face of the specimens.
247 The back face of the sample was covered by a wire mesh to protect the
248 instrumentation in case of rear-face spalling (which had been observed in similar
249 prior testing at Edinburgh (Hulin et al., 2015). Two magnetic clamps held the cross
250 bar for the displacement gauge, as shown in Figure 5, and a camera was used to
251 record the displacement gauge reading for later transcription.

Figure 6 shows H-TRIS in its warmup and test preparation phase. To protect each sample during warmup of the radiant panels until they reached a steady-state heat flux condition, insulation was placed in front of the specimens. Upon reaching a homogenous heat flux, the tests were initiated by removing the protective insulation board. Each test was programmed to follow a specific time versus incident heat flux curve (as shown in Figure 7). Two different heating curves were used: (1) an ISO 834 (2002) equivalent fire curve; and (2) a modified hydrocarbon (HCM) (BS EN 1991-1-2, 2002) equivalent heating curve. To follow these curves a calibration curve was used to guide the location of the H-TRIS radiant panels as they moved towards the test specimen. For calibration curve 1, the heat flux gauge was placed in line with the centre of the four-panel heating assembly. For calibration curve 2, the heat flux gauge was placed in line with the centre of one of the four radiant panels from which the overall radiant panel array was fabricated. Following the completion of each test, each sample was weighed, allowing the calculation of moisture lost during testing (note that no mass was lost due to spalling, since no spalling was observed for any of the samples).

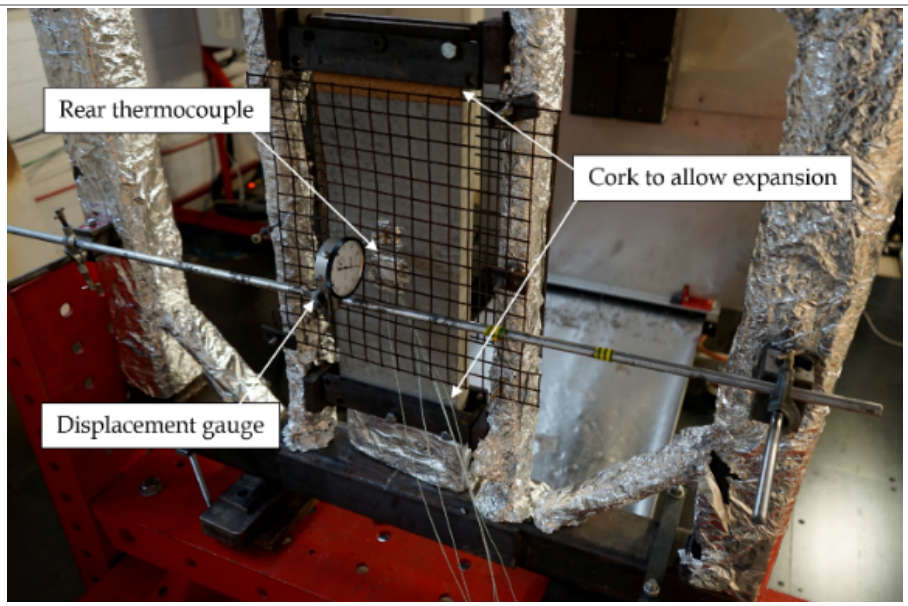

268

269 **Figure 5:** ***Restraint conditions and displacement gauge arrangement for concrete sample testing in H-***

270 ***TRIS.***

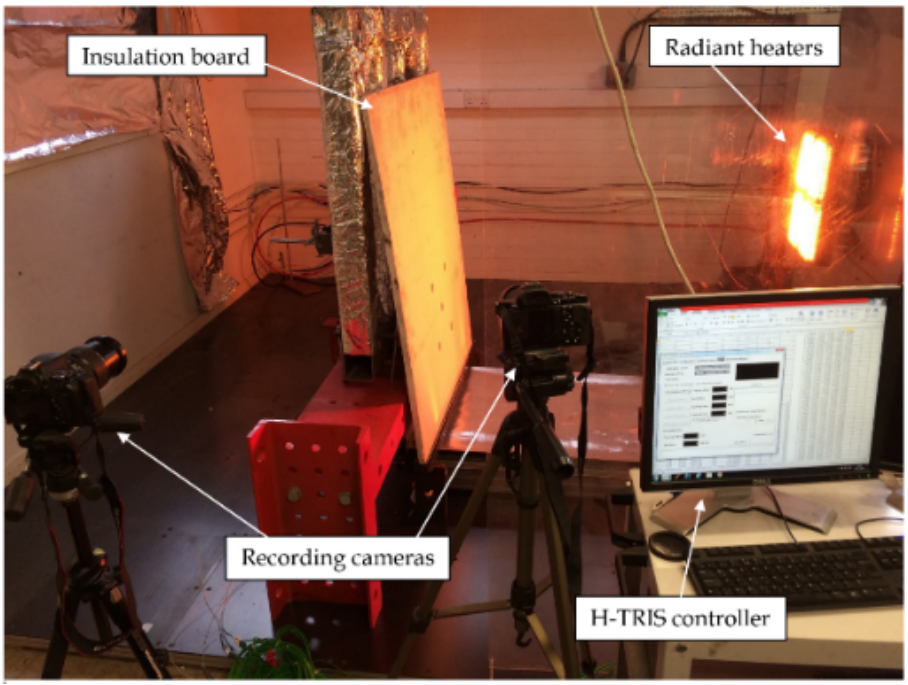

271

272 **Figure 6:** ***H-TRIS preparation phase, showing radiant panel array (left) and protective insulation board***

273 ***(centre).***

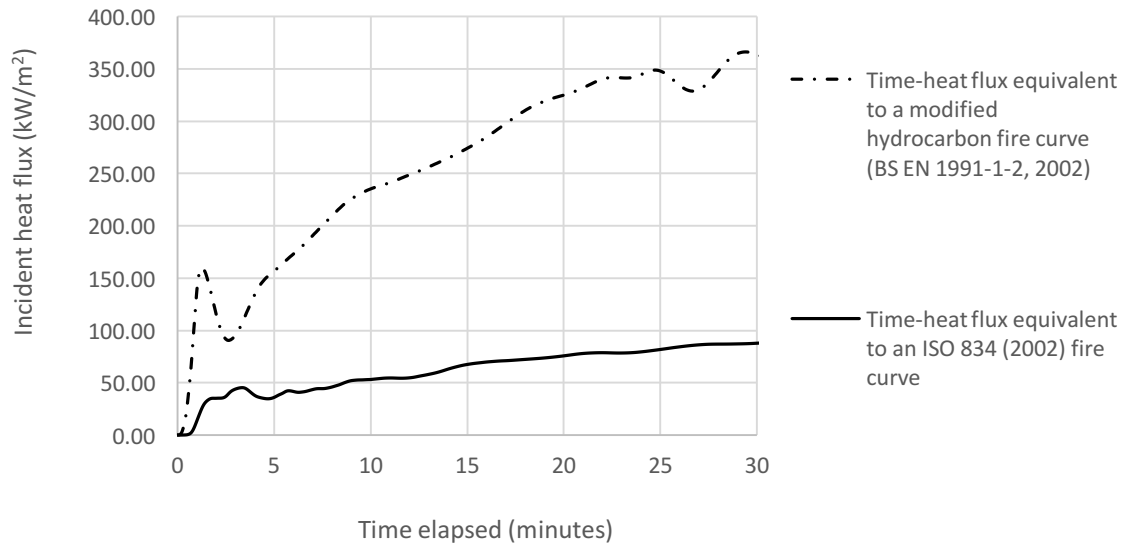

Figure 7: Time versus incident heat flux equivalent curves used for testing to both ISO and HCM heating curves.

4 Test results

4.1 Concrete properties

The average concrete compressive strength, measured from three cubes and tested in accordance with BS EN 12390-3 (2009a), was 68MPa on the test date (90 days after casting).

Table 3: ***Mass and calculated elastic modus of each concrete test sample.***

Sample name	Mass 48 hours after casting (kg)	Calculated unit mass (kg/m^3)
AT2	10.857	2412.67
AT3	11.238	2497.33
AT4	11.489	2553.11
AF2	11.099	2466.44
AF3	10.976	2439.11
AF4	11.017	2448.22

4.2 H-TRIS testing results

Table **4** summarises the results from all H-TRIS tests; as already noted, no spalling was observed for any of the samples.

288
289

Table 4**:** ***Summary of H-TRIS results***

Sample	**Concrete mix**	**Timber /fabric face**	**Equivalent heating curve (see** Figure)	**Calibration curve (see** Error! Reference source not found.**)**	**Minimum sample distance (mm)**	**Max heat flux (kW/m^2)**	**Spalling observed**	**Heating time recorded (minutes)**	**Cooling time recorded (minutes)**	**Comments**
AT2	A	Timber	ISO 834 standard fire	1	195	88	None	30	0	All thermocouples working correctly. Peak displacement estimated, no full displacement/ time data.
(AT3)	A	Timber	Modified hydrocarbon fire	1	48	197	None	7	N/A	Test failed after 7 minutes due to maximum heat flux required by heating curve exceeding maximum calibrated heat flux from the selected calibration curve. Displacement gauge failure. Data incomplete.
AT3 Retest	A	Timber	Modified hydrocarbon fire (max 162 kW/m^2)	1	97	162	None	30	0	All thermocouples working correctly. Specimen starting temperature around 70°C due to re-test. Displacement data incomplete.
AT4	A	Timber	Modified hydrocarbon fire	2	96	180	None	25	35	H-TRIS malfunction after around 25 minutes of heating. Further heating aborted. All thermocouples working correctly.
AF2	A	Fabric	Modified hydrocarbon fire (max 162 kW/m^2)	2	102	162	None	30	30	All thermocouples working correctly. Full data set collected.
AF3	A	Fabric	Modified hydrocarbon fire	2	96	180	None	25	30	H-TRIS malfunction after around 25 minutes of heating. Further heating aborted. All thermocouples working correctly.
AF4	A	Fabric	ISO 834 standard fire	1	195	88	None	30	0	5mm thermocouple not functioning.

290 N.B. 5mm temperature recordings for sample AF3 featured occasional sporadic jumps and so data has been selectively removed from
291 Figure 9 and Figure 10.

4.2.1 Temperature readings

The recorded temperatures from selected H-TRIS tests are shown in Figure 8 to Figure 10.

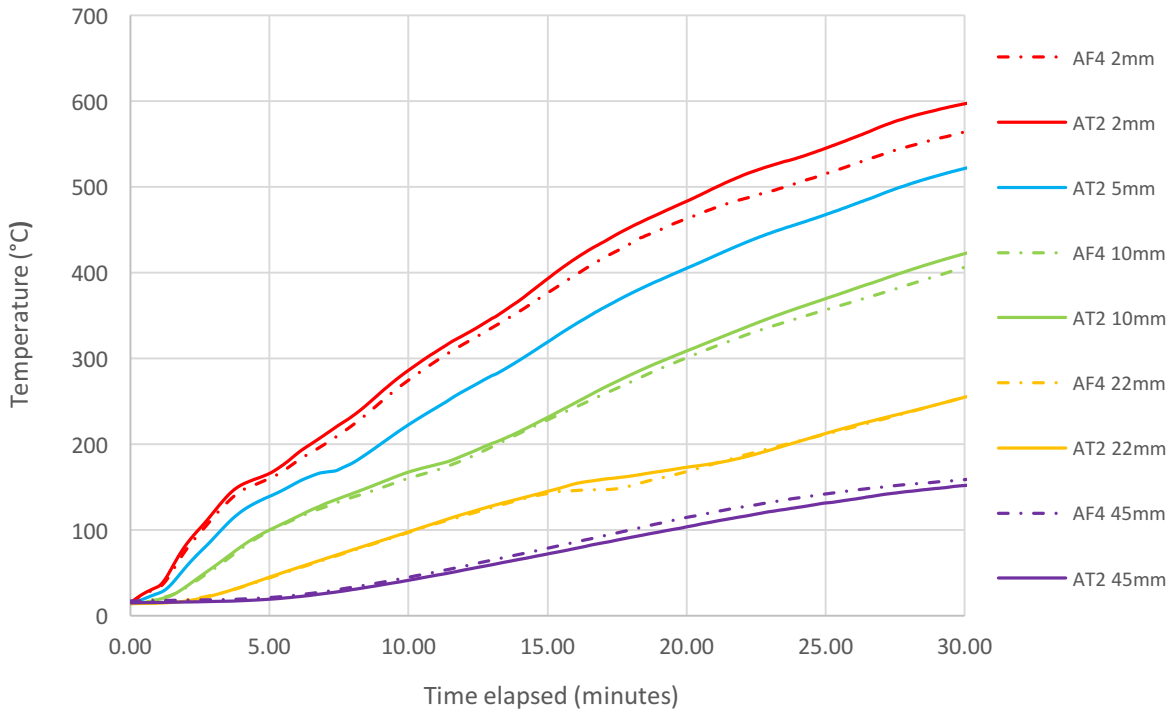

Figure 8: Temperatures recorded in H-TRIS tests on *AT2 and AF4 (simulated ISO 834 heating)*

Figure 8 shows similar and comparable temperature curves from both the traditionally cast sample, AT2, and the sample formed using a permeable mould, AF4. The front thermocouples, cast at 2mm (+/- 2mm) display a small difference in temperature most likely due to human error from placement. At the middle of both sections, 22mm (+/-2mm), temperature readings are consistent with one-another. The rear face thermocouples display alike readings.

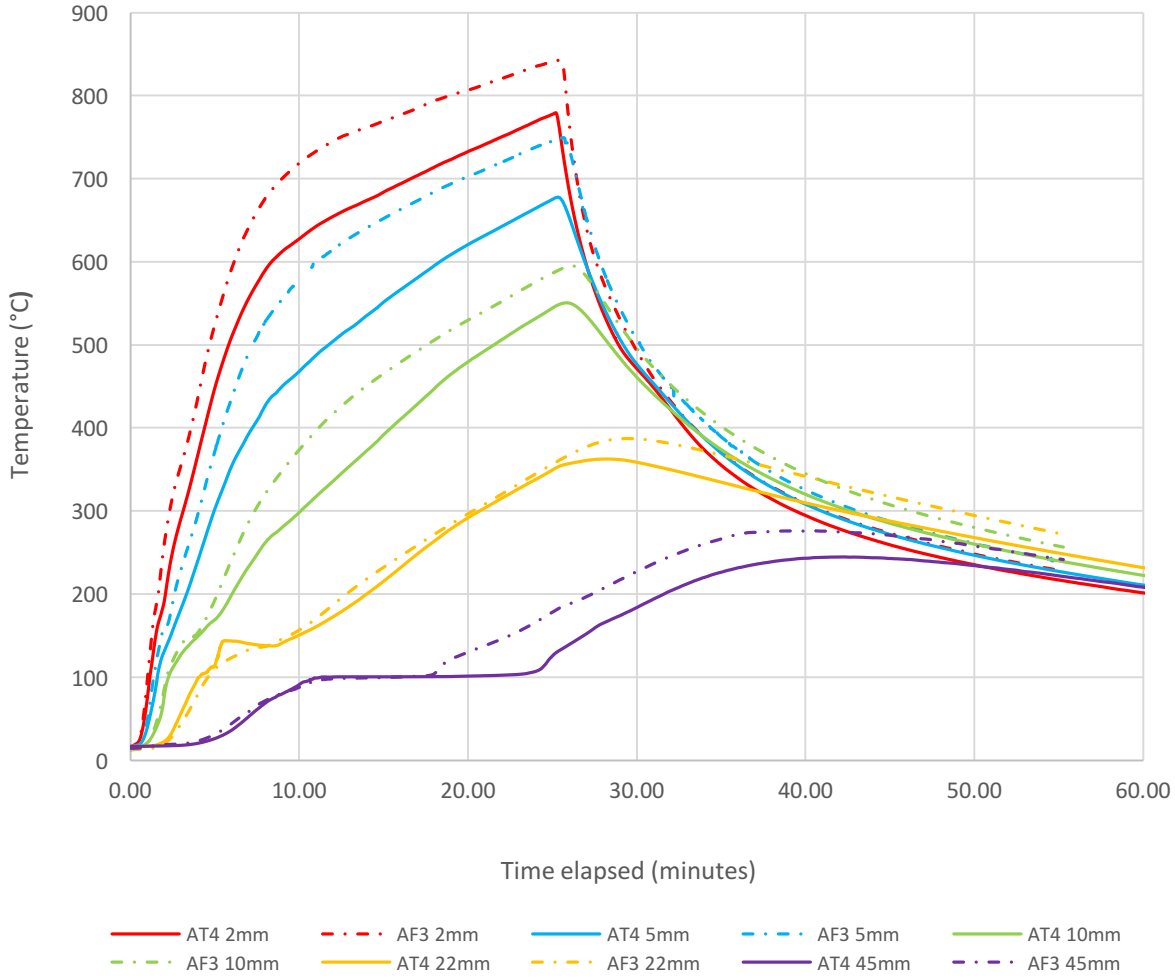

Figure 9: Temperatures recorded in H-TRIS tests *AT4 and AF3 (simulated HCM heating up to 162 kW/m^2)*

Figure 9 shows that at all thermocouple depths, temperatures are greater within the sample formed from a permeable mould, AF3, than the sample formed from traditional timber shuttering, AT4. This data suggests that the whole thermocouple tree from sample AF3 is positioned closer to the thermally loaded surface than AT4, or the thermocouple tree from AT4 is positioned further away from the thermally loaded surface than AF3.

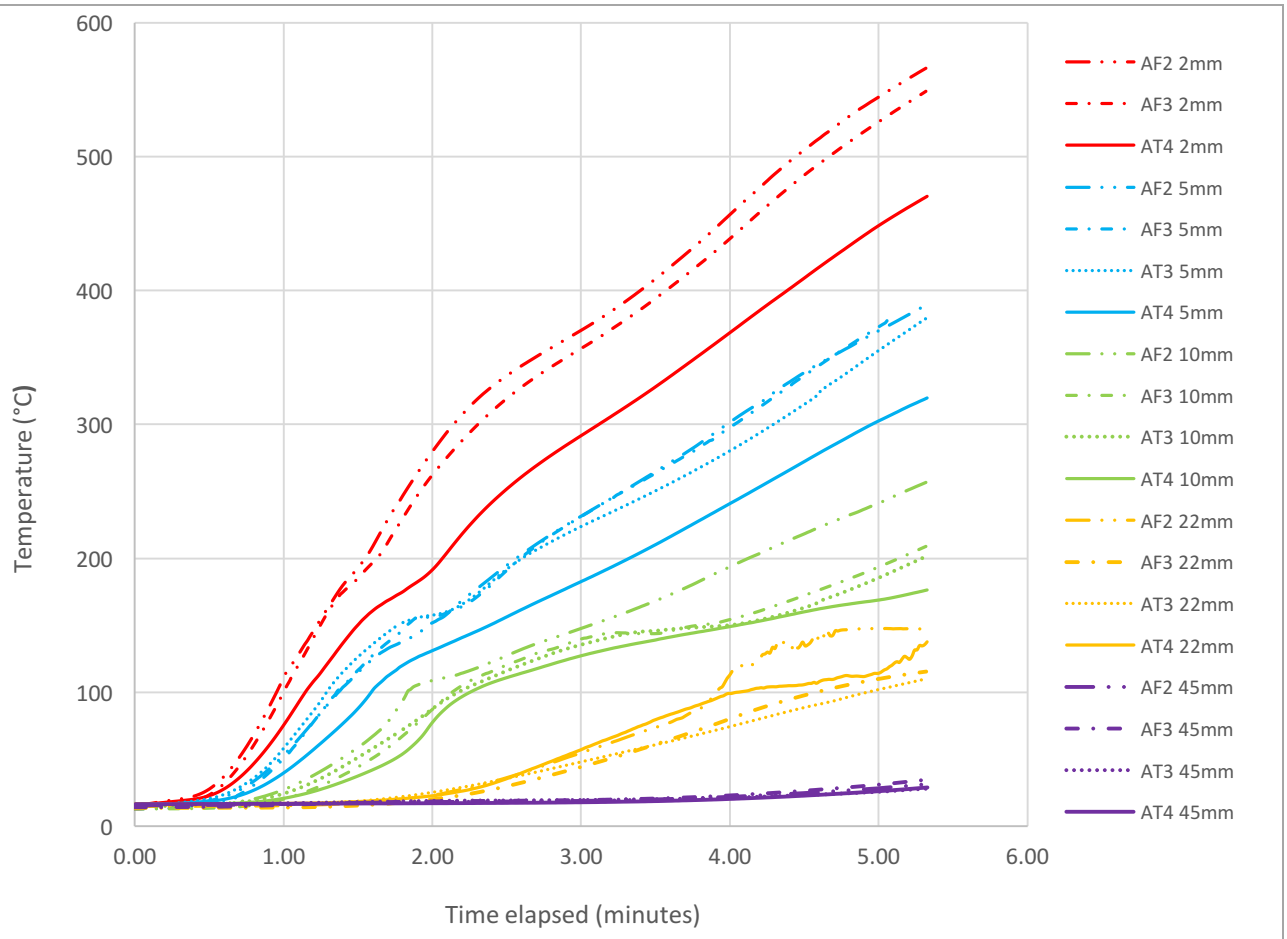

Figure 10 Temperatures recorded during H-TRIS testing on *AT3*, *AT4*, *AF2* and *AF3* (simulated HCM fire up to 162 kW/m^2)

Figure 10 incorporates temperature data from two samples formed from permeable moulds and from two traditionally cast samples. Similarly to Figure 9, permeably formed samples reach greater temperatures when studying the output from the 2mm, 5mm and 10mm (+/- 2mm) thermocouples. This trend does not continue with temperature readings from the 22mm and 45mm (+/-2mm) thermocouples, suggesting human error with placement of thermocouple trees.

4.2.2 Sample displacements

All tests were performed with samples unloaded and unrestrained against curvature and end rotations. This resulted in high differential thermal stresses causing deflection (thermal bowing) of all concrete samples during heating. All concrete samples bowed outwards, i.e.

in the direction of the heat source (Figure 11). Data is presented in Figure 12). Samples AF3 and AT4 both experienced the same H-TRIS testing regime (modified hydrocarbon fire) while sample AF4 experienced a ISO 834 fire and AF2 experienced a modified hydrocarbon fire limited to 162 kW/m^2. Differences in displacement are likely due to measurement error from thermal sources.

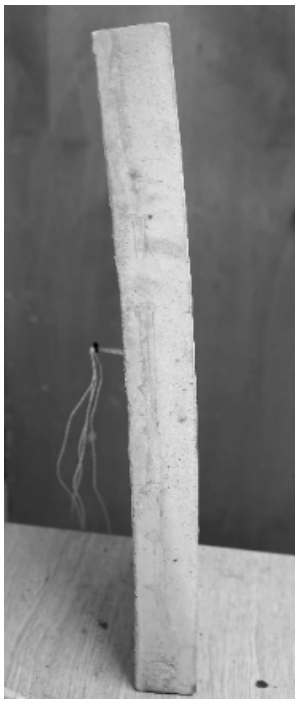

Figure 11: Post-test thermal bo*wing of Concrete Sample AT3.*

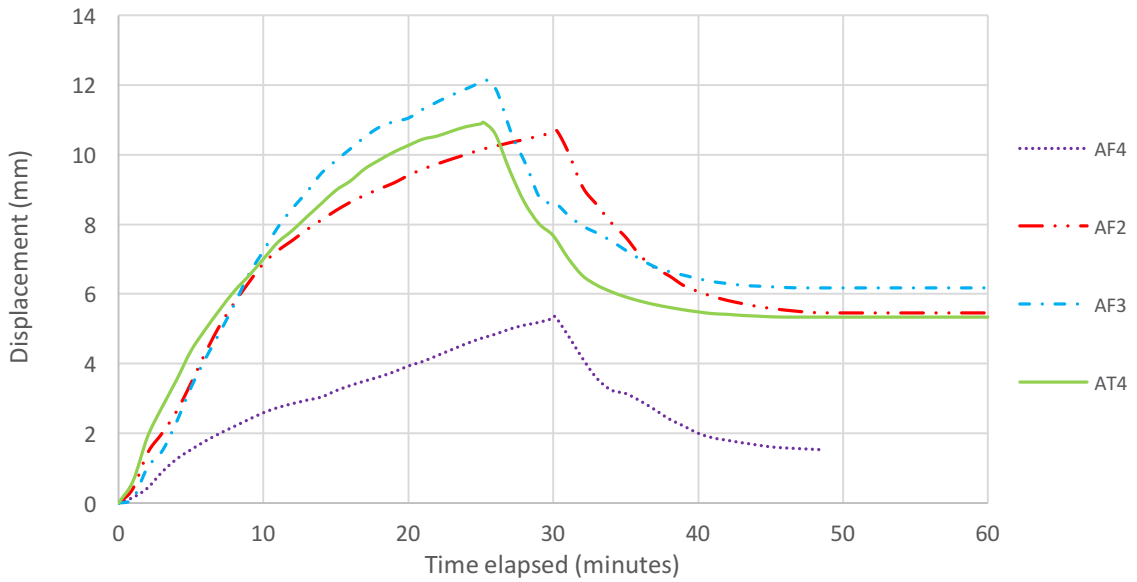

Figure 12: concrete sample *mid-height lateral displacements during heating*

4.3 Mass-loss from dehydration

Table 5 shows the mass loss from the dehydration of each sample due to fire testing. The range of specimen moisture contents lie between 5.41% and 8.41%. AT2 and AF4 have the lowest moisture content of all six samples after testing. Since these samples were exposed to the less intense ISO 834 (2002) equivalent curve, it is possible that thirty minutes of heating did not fully dry out both samples and so a value of moisture loss by mass has also been presented.

Thermal testing of 66 comparably sized specimens undertaken using H-TRIS by Maluk et al. (2013) resulted in all specimens apart from one mix set experiencing spalling. All those specimens at the time of testing had moisture contents between 4.0% to 5.0% (by mass). This comparison indicates that the moisture content of the samples tested in this paper are not dominant factors for the absence of spalling. The specimens tested by Maluk et al. (2013) had higher compressive strengths (103-112 MPa) and experienced greater restraint conditions with compressive stress applied to half of the specimens. A further discussion of factors influencing spalling such as these is presented in Section 5.

Table 5: ***Measured mass-loss from dehydration of the concrete samples during testing.***

Sample	Casting date	Mass 48 hours after casting (kg)	Post-test mass (kg)	Moisture loss by mass (%)	Moisture content (%)
AT2	09/12/2015	10.857	10.218	5.89	6.25
AT3	09/12/2015	11.238	10.366	7.76	8.41
AT4	09/12/2015	11.489	10.711	6.77	7.26
AF2	09/12/2015	11.099	10.332	6.91	7.42
AF3	09/12/2015	10.976	10.129	7.72	8.36
AF4	09/12/2015	11.017	10.452	5.13	5.41

5 Analysis

None of the samples tested showed any heat-induced explosive concrete spalling. Possible reasons for this are discussed below.

5.1 Concrete strength

Kodur and Phan (2007) stated that strengths over 70 MPa have a higher propensity to spall. Maluk et al. (2013) tested concrete samples of an identical size to those in this paper (500mm x 200mm x 45mm) using H-TRIS. High performance self-consolidating concrete (HPSCC) was used with a design strength class of C90. Out of 11 mixtures each with varying PP fibre types and quantity, four mixes spalled. This demonstrates that even with a considerably higher strength, spalling tends to display an element of randomness and is influenced by other factors in addition to the strength class, even with carefully controlled testing and thermal exposures, thus underlining a lack of understanding of the risk of spalling and the mechanisms contributing to spalling.

5.2 Restraint conditions

During testing, all samples were unrestrained at their ends. They all exhibited large bowing under heating due to the high through-thickness thermal gradient created by heating from one side of the specimen. Their lack of restraint, and ability to deform, may have contributed to the absence of spalling. Hertz (2003) demonstrated that for samples restrained in place with fixed ends, it is more difficult for specimens to relieve internal thermal stresses through deflection, making restrained specimens more likely to spall.

5.3 Applied loading

All specimens in this paper were tested without externally applied static loads. The addition of a moderate amount of compression has been shown to increase the likelihood of spalling. Carré et al. (2013) exposed specimens with a concrete strength of 37MPa to

an ISO 834 (2002) time-temperature curve. With up to a 10MPa compression on these specimens, no spalling was recorded. At 15MPa compression, spalling was observed.

5.4 Thermal cracking

A further underlying reason for the absence of spalling seen in this paper can be related to the extensive thermal cracking which developed during testing. As thermal cracks develop in normal density concrete without external load or restraint as was used here, stresses at the surface are relieved and the propensity for spalling is reduced (Hertz, 2003).

5.5 Summary

The concrete samples cast using permeable moulds do not appear to be more susceptible to spalling under the conditions studied. There are no obvious differences in the temperature profiles or thermal curvatures from H-TRIS testing indicating that the increased surface durability gained from using fabric formwork does not increase the likelihood of spalling over traditionally formed concrete given the testing conditions. Slight variances in temperature readings can be accounted for by minor differences in the cast positions of thermocouples. As no spalling was observed, an investigation into the altered pore structure from permeable mould formed samples was undertaken using scanning electron microscopy.

6 Scanning electron microscopy

To assess the porosity of concrete cast against timber and a permeable fabric, eight concrete samples of 25mm x 25mm x 25mm were cut from the centres of untested samples (four from an impermeably and four from a permeably cast sample). The cubes were set in epoxy resin under vacuum and polished to a high degree before imaging. No splutter coatings were applied to the sample. An example of a fabric formed surface sample is shown in Figure 13.

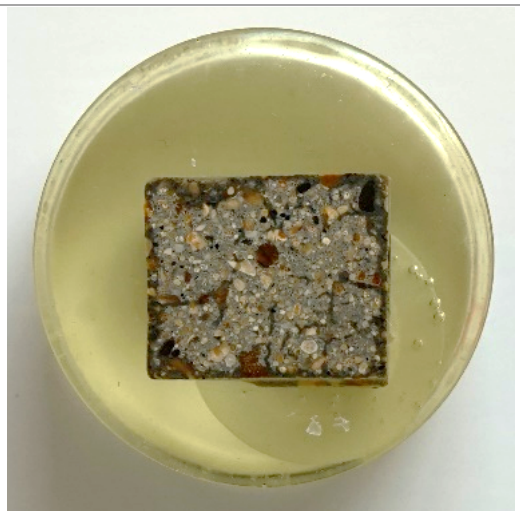

Figure 13: ***A polished fabric surface sample.***

A JEOL SEM was used at the University of Bath for imaging. A range of backscattered electron images (BEI) were captured under low vacuum mode at 300x and 500x magnification. The samples were positioned with cast surface layer (permeable mould/timber) facing up at the microscope.

6.1 Scanning electron microscopy results

BEI imaging taken from four concrete samples (permeable mould or timber: ‘a’ and ‘b’ samples taken from the same sample in different locations) are shown in Figure 14 - Figure 17. Voids are shown as black since the epoxy resin that filled the sample is very light in comparison to the concrete. Heavier minerals appear lighter. Frame positions for imaging were chosen with the aim of gathering a range of images from the cast surface layer.

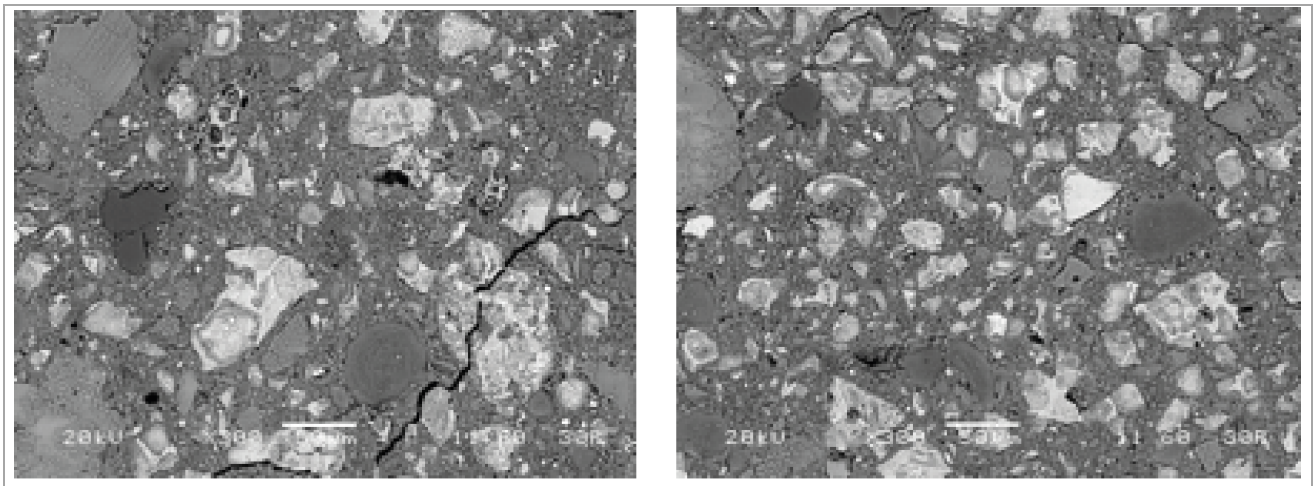

(a) (b)

414

415 **Figure 14: BEI (a, b) permeable mould surface at 300x magnification**

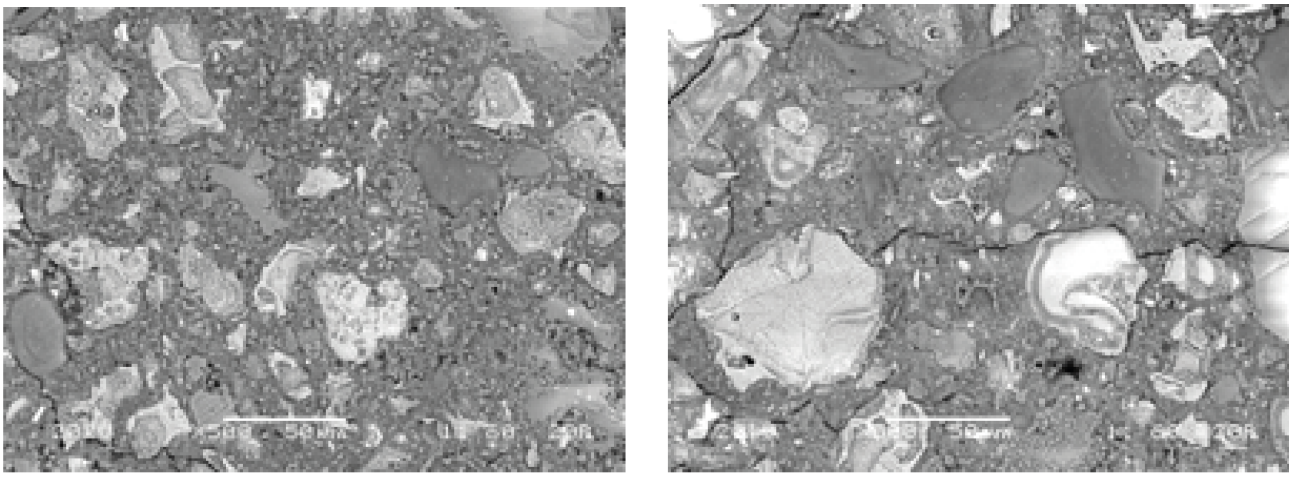

(a) (b)

416

417 **Figure 15: BEI (a, b) permeable mould surface at 500x magnification**

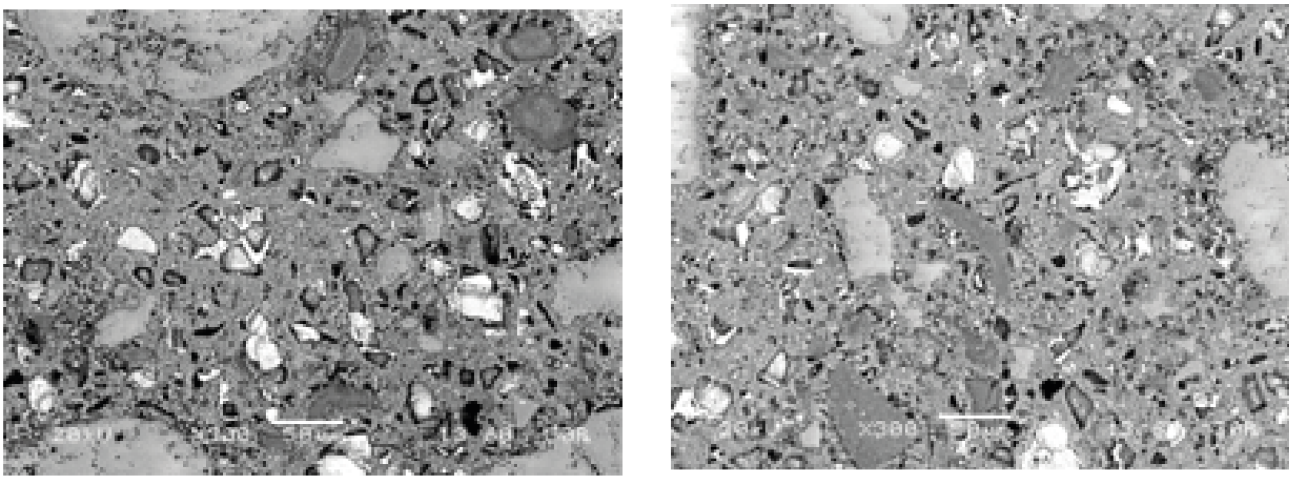

(a) (b)

418

419 **Figure 16: BEI (a, b) timber formed surface at 300x magnification**

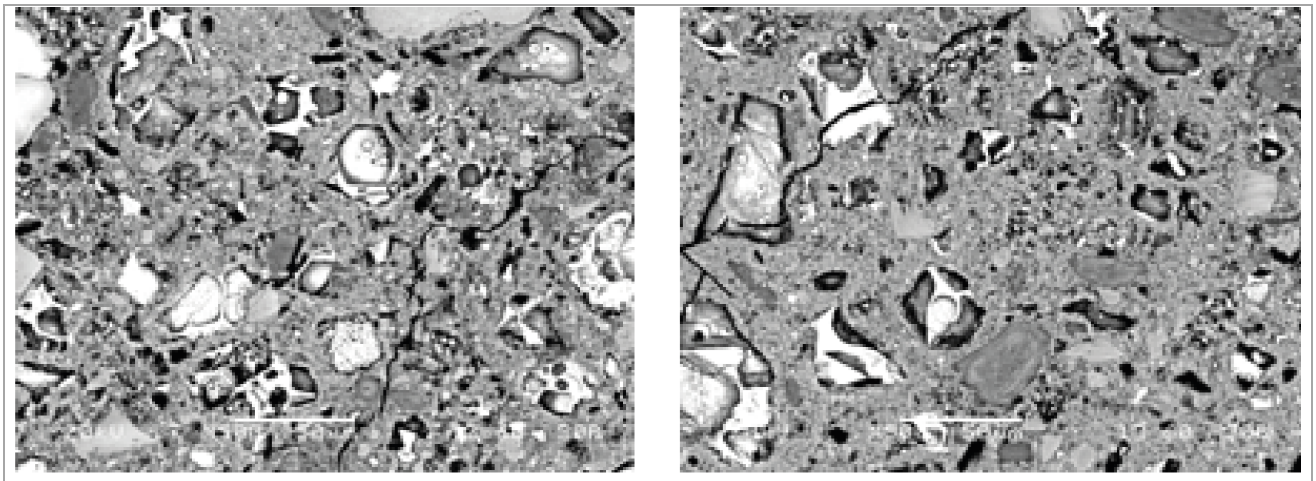

(a) (b)

420

421 **Figure 17: BEI (a, b) timber formed surface at 500x magnification**

422 *6.1.1 Image analysis*

423 'ImageJ' analysis software (Ferreira and Rasband, 2011) was used to analyse the SEM
424 imaging. To account for greyscale inaccuracies reproduced by the SEM, thresholding was
425 performed using the 'analyse particles' function. For continuity one pore was selected per
426 sample as a benchmark. To obtain a quantitative comparison of porosity, a particle
427 analysis function was used to calculate the area of voids as a frame percentage. Original
428 images were used with no cropping or removal of aggregates.

429

430

431 **Table 6:** ***Average voids radio per surface finish at 300x and 500x magnification.***

Surface finish	Magnification	Average void area (per frame as a %)
Fabric	300x	0.92
Timber	300x	3.81
Fabric	500x	0.47
Timber	500x	3.00

6.1.2 Summary

A stark difference is evident in the magnitude and distribution of pores between concrete formed from a permeable mould (Figure 14 and Figure 15) and a timber formed surface (Figure 16 and Figure 17). Table 6 shows the average voids area is over four times greater for a timber formed surface at 300x magnification, providing significant evidence of reduced porosity, and therefore, decreased permeability of a surface formed from a permeable mould. Orr et al. (2013) also demonstrated that a fabric formed surface layer contained a greater concentration of cement particles resulting in smaller and fewer interconnected pores. The higher density microstructure of the permeable mould concrete is further demonstrated by the large and frequent C-S-H gel formation, visible at 500x magnification, appearing as dark grey, by comparing Figure 15 and Figure 17).

7 Evaluation of experimentation

7.1 H-TRIS testing

Since all samples were tested unrestrained and unloaded, thermal expansion and bowing was expected. The boundary conditions tested simulate, for example, a concrete façade. To simulate a realistic structural load bearing scenario, the sample should be tested with axial and/or flexural restraint, and with representative loading applied.

7.2 Scanning electron microscopy

As a result of sample preparation, from polishing the surface of both the permeable mould and timber formed samples, the texture of the true outer layer was partially lost, and therefore, the backscattered electron images do not represent the exact surface layer. Section 6.1 still shows a distinct difference in the imaged surface layers and so, in the Author's opinion, the validity of the conducted microscopy remains.

8 Conclusions

The additional density and restricted permeability found by Orr et al. (2013) at the surface layer of fabric formed concrete revealed a potential hazard for the fire related performance of fabric formed concrete, specifically with relation to heat-induced explosive concrete spalling.

A pilot study, presented in this paper, was undertaken to examine this potential hazard. Fire testing undertaken at the University of Edinburgh using H-TRIS was inconclusive, with no observed spalling for concrete samples cast using conventional formwork or using permeable fabric formwork. Further research is required to draw definitive conclusions, either replicating the boundary conditions of testing undertaken in this paper (to simulate a concrete façade) or with structural restraint conditions and applied loading to the samples to replicate likely behaviour in service, such as a concrete wall.

Scanning electron microscopy was performed to investigate the porosity of the cast samples. The image analysis performed supports the prior results from Orr et al. (2013), concluding that the studied fabric formed surface layer featured considerably lower porosity (over four times less porous) than the given timber formed layer.

With evidence showing the porosity of permeable mould formed surfaces to be lower (and thus, reducing the permeability of the surface, identified as a spalling hazard), it is recommended that further research be conducted on this topic.

9 Further research

Determining the effect on spalling of permeable moulds requires additional research. The non-spalling results found in this paper should not be extrapolated beyond the specific boundary conditions of the samples tested.

Fabrics with a range of pore sizes should be investigated, as the permeability of the mould is linked to the permeability of the cast concrete by the curing process.

Further testing to the same incident heat flux – time thermal exposures is recommended, on specimens with restrained end conditions to prevent bowing, and an applied compression load, to more realistically represent in-service fabric formed concrete. Determining the fire performance of permeably cast concrete remains an important research question to answer.

10 Acknowledgments

The authors wish to acknowledge the Building Research Establishment Centre for Fire Safety Engineering (University of Edinburgh), Microscopy and Analysis Suite (University of Bath) and laboratory staff from the Department of Architecture and Civil Engineering (University of Bath). CEMEX are gratefully acknowledged for providing mix design guidance and silica fume.

11 Data access statement

All data created in this paper are openly available from the data archive at http://doi.org/10.10125/CAM (TBC).

12 References

ASTM 2016. E119. *Standard Test Methods for Fire Tests of Building Construction and Materials.* West Conshohocken, PA: ASTM International.

BSI 2004. BS EN 1992-1-2. *Eurocode 2: Design of Concrete Structures - Part 1-2: General Rules - Structural Fire Design.* London: BSI.

BSI 2009a. BS EN 12390-3. *Testing hardened concrete. Part 3: Compressive strength of test specimens.* London, UK: BSI.

BSI 2009b. BS EN 13670. *Execution of concrete structures.* London: BSI.

CARRÉ, H., PIMIENTA, P., LA BORDERIE, C., PEREIRA, F. & MINDEGUIA, J. C. 2013. Effect of compressive loading on the risk of spalling. *MATEC Web of Conferences.*

CHANDLER, A. & PEDRESCHI, R. 2007. *Fabric Formwork,* London, RIBA.

FERREIRA, T. & RASBAND, W. 2011. *ImageJ User Guide,* Maryland, National Institutes of Health.

FRANK 2015. Zemdrain Controlled permeability formliner. Leiblfing Germany: DuPont.

GROSSHANDLER, W. 2002. NISTIR 6890 – Fire Resistance Determination and Performance Prediction Research Needs Workshop. Gaithersburg: National Institute of Standards and Technology.

HARMATHY, T. Z. 1965. Effect of moisture on the fire endurance of building materials. *ASTM Special Technical Publication,* Moisture in Materials in Relation to Fire Tests**,** 74-95.
HAWKINS, W. J., HERRMANN, M., IBELL, P. T., KROMOSER, B., MICHAELSKI, A., ORR, J. J., PRONK, A., SCHIPPER, R., SHEPHERD, P., VEENENDAAL, D., WANSDRONK, R. & WEST, M. 2016. A state of the art review of flexible formwork technologies. *Structural Concrete*.
HERTZ, K. D. 2003. Limits of spalling of fire-exposed concrete. *Fire Safety Journal,* 38**,** 103–116.
HERTZ, K. D. & SØRENSEN, L. S. 2004. Test method for Spalling of Fire Exposed Concrete. *Fire Safety Journal,* 40**,** 466-476.
HULIN, T., MALUK, C., BISBY, L., HODICKY, K., SCHMIDT, J. W. & STANG, H. 2015. Experimental studies on the fire behaviour of high performance concrete thin plates. *Fire Technology,* 52.
ISO 2002. ISO 834-8. *Fire-resistance tests -- elements of building construction -- part 8: Specific requirements for non-loadbearing vertical separating elements.* ISO.
JANSSON, R. 2008. *Material properties related to fire spalling of concrete.* Licentiate thesis, LUND INSTITUTE OF TECHNOLOGY.
JANSSON, R. 2013. *Fire Spalling of Concrete.* Doctoral thesis, Sweden.
KHOURY, G. A. 2000. Effect of fire on concrete and concrete structures. *Progress in Structural Engineering and Materials,* 2**,** 429–447. .
KLINGSCH, E. W. H. 2014. *Explosive Spalling of Concrete in Fire.* PhD thesis, ETH Zurich.
KODUR, V. K. R. & PHAN, L. 2007. Critical factors governing the fire performance of high strength concrete systems. *Fire Safety Journal,* 42**,** 482–488.
LAWSON, J. R., PARKER, A. & DEAN, S. W. 2009. A history of fire testing: Past, present, and future. *Journal of ASTM International,* 6.
LURA, P. & TERRASI, G. P. 2014. Reduction of fire spalling in high-performance concrete by means of superabsorbent polymers and polypropylene fibers. *Cement and Concrete Composites,* 49**,** 36–42.
MALUK, C. & BISBY, L. 2012. 120 years of structural fire testing: Moving away from the status quo. . *2nd Fire Engineering Conference.*
MALUK, C., BISBY, L., KRAJCOVIC, M. & TORERO, J. L. 2016. A Heat-Transfer Rate Inducing System (H-TRIS) Test Method. *Fire Safety Journal*.
MALUK, C., BISBY, L., TERRASI, G., KRAJCOVIC, M. & TORERO, J. L. 2012. Novel Fire Testing Methodology: Why, how and what now? . *Proceedings of the Mini Symposium on Performance-based Fire Safety Engineering of Structures.*
MALUK, C., BISBY, L. & TERRASI, G. P. 2013. Effects of polypropylene fibre type on occurrence of heat-induced concrete spalling. *MATEC Web of Conferences.*
MINDEGUIA, J.-C., PIMIENTA, P., HAGER, I. & CARRÉ, H. 2011. INFLUENCE OF WATER CONTENT ON GAS PORE PRESSURE IN CONCRETES AT HIGH TEMPERATURE.
ORR, J. J., DARBY, A. P., IBELL, P. T. & EVERNDEN, M. 2013. Durability enhancements using fabric formwork. *Magazine of Concrete Research,* 65**,** 1236-1245.
ORR, J. J., DARBY, A. P., IBELL, T. J., EVERNDEN, M. C. & OTLET, M. 2011. Concrete structures using fabric formwork. *The Structural Engineer,* 89**,** 20-26.
PRICE, W. F. 2000. Controlled permeability formwork. London: Construction Industry Research and Information Association.
RICKARD, I., GERASIMOV, N., BISBY, L. & DEENY, S. 2017. Predictive testing for heat induced spalling of concrete tunnel linings - The potential influence of sustained mechanical loading. *In:* BOSTROM, L. & JANSSON MCNAMEE, R. (eds.)

Proceedings from the 5th International Workshop on Concrete Spalling. Boras, Sweden: RISE Research Institutes of Sweden.
VEENENDAAL, D., WEST, M. & BLOCK, P. 2011. History and overview of fabric formwork: using fabrics for concrete casting. *Structural Concrete,* 12**,** 164-177.
ZEIML, M., LEITHNER, D., LACKNER, R. & MANG, A. 2006. How do polypropylene fibers improve the spalling behavior of in-situ concrete? *Cement and Concrete Research,* 36**,** 929-942.
ZHANG, H. & DAVIE, C. 2013. A numerical investigation of the influence of pore pressures and thermally induced stresses for spalling of concrete exposed to elevated temperatures. *Fire Safety Journal,* 59**,** 102-110.